Electron Diffraction Investigation on the Molecular Structure of n-Butane

By Kôzo KUCHITSU

(Received December, 27, 1958)

The structural parameters of normal hydrocarbons have not yet been thoroghly studied[1], except the simplest ones, methane[2] and ethane[3-5], though there are many investigations on their halogen derivatives[6]. The results which have so far been obtained, except the above two, are on propane by Pauling and Brockway[7], C–C=1.54±0.02A, and ∠C–C–C=111.5°±3°, and on *n*-butane by Wierl[8], C–C=1.51± 0.05A. As the technique has since been developed, more accurate results are expected to be given in the determination of the C–C distances and the C–C–C valence angles. Furthermore, the position of hydrogen atoms may be located with considerable accuracy, because these molecules do not include heavier atoms than carbon. Accordingly, it seems worth while to investigate the structure of *n*-butane.

Various spectroscopic and thermodynamic studies have shown that rotational isomers exist in the normal paraffins higher than propane[6]. As for *n*-butane, it was first noticed by Kohlrausch and Köppl[9] in their study of the Raman spectra. It was soon confirmed by Mizushima, Morino and Nakamura[10] in their study of the Raman spectra in the liquid and solid. They found that two forms exist in the liquid whereas only the *trans* form remains in the solid. The energy difference between the isomers was measured by Szasz and his co-workers in the liquid phase[11,12]. They obtained from the measurement of the temperature dependence of the Raman intensity the value of 770±90 cal./mol.[11], or 760±100 cal./mol.[12] (the *trans* form being the more stable). This result is in good agreement with the value of 800 cal./mol. which was estimated by Pitzer[13] from the entropy of *n*-butane[14] and used in the studies of the thermodynamic functions of hydrocarbons. Thus the rotational isomerism seems to be well established in the liquid phase, but no experimental evidence concerning the energy difference in the vapor is so far available[12]. While it seems probable that the magnitude is nearly the same as in the liquid because of the nonpolar nature of the molecule, the infrared spectrum of the vapor of *n*-butane was interpreted by Gates[15] in terms of a single form. However, as pointed out by Axford and Rank[16], his interpretation seems to rest on a rather insecure foundation and a further study on this point will make the situation clear. In the present study it is confirmed that two isomers exist, the *trans* and the *gauche* forms, in the vapor of *n*-butane, the energy difference being nearly equal to that in the liquid.

Experimental

The electron diffraction instrument used in this study was designed by Morino, Kimura and Iwasaki[17]. The details of the apparatus and procedure were reported previously[18-20]. Diffraction photographs were taken through an r^3-sector

1) M. H. Jellinek, "Physical Chemistry of Hydrocarbons," Vol. I, Chap. 2, Academic Press Inc., New York (1950).
2) G. Herzberg, "Infrared and Raman Spectra of Polyatomic Molecules", D. Van Nostrand Co., Inc., New York (1945).
3) G. E. Hansen and D. M. Dennison, *J. Chem. Phys.*, **20**, 313 (1952).
4) K. Hedberg and V. Schomaker, *J. Am. Chem. Soc.*, **73**, 1482 (1951).
5) A. Almenningen and O. Bastiansen, *Acta Chem. Scand.*, **9**, 815 (1955).
6) S. Mizushima, "Structure of Molecules snd Internal Rotation", Academic Press Inc., New York (1954).
7) L. Pauling and L. O. Brockway, *J. Am. Chem. Soc.*, **59**, 1223 (1937).
8) R. Wierl, *Ann. Physik*, **13**, 453 (1932).
9) K. W. F. Kohlrausch and F. Köppl, *Z. phys. Chem.*, **B26**, 209 (1934).
10) S. Mizushima, Y. Morino and S. Nakamura, *Sci. Papers Inst. Phys. Chem. Research (Tokyo)*, **37**, 205 (1940).
11) G. J. Szasz, N. Sheppard and D. H. Rank, *J. Chem. Phys.*, **16**, 704 (1948).
12) N. Sheppard and G. J. Szasz, ibid., **17**, 86 (1949).
13) K. S. Pitzer, ibid., **5**, 473 (1937).
14) K. S. Pitzer, ibid., **8**, 711 (1940); *J. Am. Chem. Soc.*, **63**, 2413 (1941).
15) D. M. Gates, *J. Chem. Phys.*, **17**, 393 (1949).
16) D. W. E. Axford and D. H. Rank, ibid., **18**, 51 (1950).
17) Y. Morino, M. Kimura and M. Iwasaki, The Sixth Annual Meeting of the Chemical Society of Japan (1953).
18) T. Ino, *J. Phys. Soc. Japan*, **8**, 92 (1953).
19) Y. Morino and K. Kuchitsu, *J. Chem. Phys.*, **28**, 175 (1958).
20) Y. Morino, K. Kuchitsu and E. Hirota, "Electron Diffraction by Gas", Maruzen Co., Tokyo (1957).

(in the case of the shorter camera length, 11.8 cm.) or an r^2-sector (in the case of the longer camera length, 27.9 cm.). The sectors were carefully cut to fit the proper shape within a hundredth of a millimeter[21]. They were mounted on a ball-bearing race and rotated rapidly during the exposure. In taking the diffraction photographs particular care was taken in regard to the constancy of the electron wavelength, the reducing of the extraneous scattering, and a good localization of the sample vapor.

The electron beam was focused to a spot of about 0.1 mm. in diameter. The fluctuation or the drift of the accelerating voltage was regulated within 0.1%. The wavelength of the beam was determined to be about 0.0556Å by a transmission pattern of gold foil. In order to reduce the extraneous scattering, a beam stopper of a shape similar to that described by Brockway[22] or Bastiansen[23] was mounted at the center of the sector[21]. The effect of the stopper on reducing the extraneous background was clearly seen on the photometer trace; the blank line of the photometer curve was nearly on the same level as the center line screened by the stopper, illustrating the fact that the extraneous background was not significant. Further evidence was given by a "blank test"[24] (taking photographs under the same condition as the experiment but without a sample jet), or by the "shadow test"[24] (taking photographs with the sample jet through a non-rotating sector) showing that there was no appreciable extraneous scattering caused by the main beam, nor by the scattering on the edge of the sector, of the slit, and of the nozzle aperture.

A "Research Grade" sample of *n*-butane of Phillips Petroleum Company was kindly furnished by Mr. T. Takatani of the Hitachi Central Research Laboratory. The sample (gas at room temperature) was introduced into a glass container of about 1 liter and the pressure was kept at about 20 mmHg. A liquid air trap was placed just over the nozzle to prevent the sample from diffusing through the camera. The flowing rate of the sample gas was carefully controlled, and diffraction photographs were taken with a long exposure time (a few minutes)[23,25]. A set of three photographs of different exposures were taken successively and developed at one time in the same bath. Two of the better photographs among them were used for the density-intensity calibration.

The photographs were scanned by a Riken B-type recording microphotometer of Nagoya University to measure the optical density as a function of the radius[18]. The photographic plate was rotated rapidly about the center of the pattern while being scanned by the photometer.

The measurement of the photometer curves was carried out with a Riken two-dimensional comparator in the interval of $\Delta q=0.5$. Optical densities thus measured were converted into relative intensities either by Karles' method[26] or by Bartell's method[27] by using the set of two density curves. The resulting intensity curves were averaged respectively for each set. The agreement between the calibration curves obtained by either method was satisfactory. The curves obtained in both procedures were used in the analysis described below.

The averaged intensity curve was multiplied by $q^{1/2}$ to accentuate the molecular oscillations, and a smooth background line I_B was drawn through the curve. After a few steps of redrawing of the line, a reasonable background which satisfies Karles' criterion[24,26], that is, no fluctuation (0.0 through 0.7Å) and non-negativeness of the baseline of the radial distribution curve was obtained. The corresponding molecular intensity curve $qM(q)$ was readily calculated by using the following equation[26]:

$$qM(q)=q(I/I_B-1) \tag{1}$$

The above procedures were repeated one by one for the three sets of plates taken with the shorter camera length, and finally five molecular intensity curves shown in Fig. 1 were obtained: two from the curves calibrated by Karles' procedure, two by Bartell's procedure, and one for which the density is nearly linear so that the same molecular intensity curve was obtained by both calibrations. The average deviations of the peak positions and intensities, listed in Table I,

TABLE I. AVERAGE DEVIATIONS OF THE PEAK POSITIONS AND INTENSITIES FOR FIVE OBSERVED MOLECULAR INTENSITY CURVES

Peak		Peak position[a]		Peak intensity[b]	
Max.	Min.	Average	Average dev.	Average	Average dev.
3		18.18	0.08	1.37	0.06
	3	23.02	0.06	−0.22	0.04
4		28.18	0.06	1.12	0.06
	4	35.07	0.04	−2.95	0.14
5		41.08	0.02	3.05	0.18
	5	50.19	0.07	−1.70	0.08
6		56.55	0.04	2.10	0.10
	6	61.31	0.05	−1.28	0.05
7		67.84	0.06	0.80	0.04
	7	75.14	0.09	−0.79	0.03
8		80.92	0.14	1.08	0.02
	8	87.60	0.16	−0.93	0.04
9		95.03	0.14	0.89	0.04
Average		—	0.08	—	0.07

a) in q-unit.
b) in absolute unit.

21) S. Shibata, Symposium on the Diffraction of X-ray and Electrons (1955).
22) L. O. Brockway and L. S. Bartell, *Rev. Sci. Instr.*, **25**, 569 (1954).
23) O. Bastiansen, O. Hassel and E. Risberg, *Acta Chem. Scand.*, **9**, 232 (1955).
24) I. L. Karle and J. Karle, *J. Chem. Phys.*, **18**, 963 (1950).
25) O. Bastiansen, L. Hedberg, and K. Hedberg, ibid., **27**, 1311 (1957).
26) J. Karle and I. L. Karle., ibid., **18**, 957 (1950).
27) L. S. Bartell and L. O. Brockway, *J. Appl. Phys.*, **24**, 656 (1957).

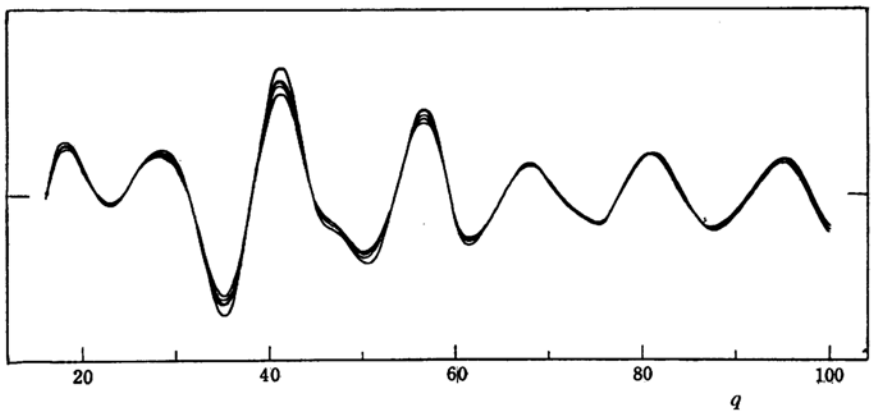

Fig. 1. Experimental molecular intensity curves for *n*-butane. Five experimental intensity curves are given in the same coordinate. The maximum average deviations among these intensities (near $q=40$) amounts to about 6%.

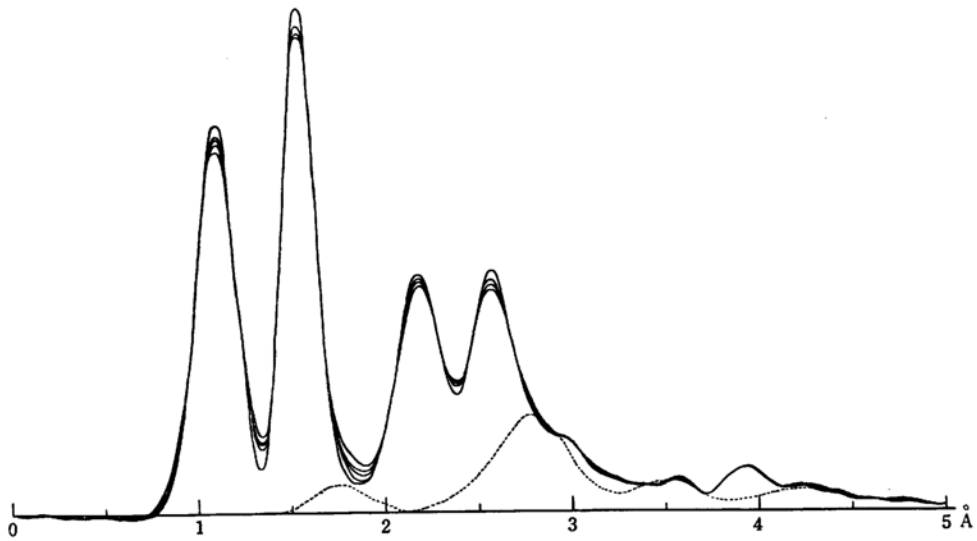

Fig. 2. Experimental RD curves. The RD curves computed from the five experimental intensity curves (Fig. 1) are illustrated in the same scale. The average deviations at the larger peaks are 1~2%. The dotted line denotes a minor contribution from the atomic pairs including hydrogen computed by use of a self-consistent model (see text). It is seen that the curves are non-negative everywhere within the experimental uncertainty.

are important measures for estimating the experimental errors of the structure analysis.

Analysis of the Radial Distribution Curve

Procedure.—Modified radial distribution curves[28] (they will be abbreviated as RD curves) were calculated from the molecular intensity curves, changing the Fourier integral into summation[29,30],

$$f(r)=\sum_{q=1}^{100} qM_c(q)\sin(\pi qr/10)\exp(-b\pi^2q^2/100) \quad (2)$$

where $qM_c(q)$ is the observed molecular intensity corrected for the non-nuclear scattering. Since the experimental intensity extends to $q=100$, a constant b was chosen to be 0.002333 to make the summation converge rapidly.

The summation was performed by the use of a punched-card machine[29]. The detail of the computation was given elsewhere[31]. Near the end of the study, a

28) Y. Morino and E. Hirota, *J. Chem. Phys.*, 28, 185 (1958).
29) P. A. Shaffer, V. Schomaker and L. Pauling, ibid., 14, 648, 659 (1946).
30) T. Ino, *J. Phys. Soc. Japan*, 12, 495 (1957).
31) Y. Morino and K. Kuchitsu, *X-Rays*, 8, 37 (1954).

TABLE II. SELF-CONSISTENT ANALYSIS FOR THE STRUCTURE (in Å unit)

Atomic pair	A		B		C	
	Distance	Mean amplitude	Distance	Mean amplitude	Distance	Mean amplitude
C-H	1.090	0.078	1.092	0.0830	1.092	0.0823
C-C	1.540	0.050	1.540	0.0534	1.539	0.0530
C-H (nonbonded)	2.163	0.110	2.178	0.1075	2.179	0.1005
C-C (nonbonded)	2.515	0.070	2.552	0.0739	2.553	0.0726
C-C (*gauche*)	2.949	0.160	(3.047)[a]	(0.160)[a]	3.12	0.125
C-C (*trans*)	3.876	0.070	3.906	0.0749	3.914	0.065

A: The model assumed at the first stage.
B: Result of the first analysis.
C: Result of the second analysis.
a) The *gauche* distance and its mean amplitude could not be measured accurately in the first analysis. Therefore, the values in brackets were used as the basis of the second analysis. The distance was calculated by using the result of the first analysis and the assumption that the azimuthal angle was 60°.

parametron digital computor became available at Department of Physics of the University of Tokyo. Some of the calculations were carried out by the use of this machine[32].

The RD curves thus obtained for the five molecular intensity curves are illustrated in Fig. 2; the agreement is satisfactory. A detailed analysis was made for the averaged RD curve.

Care was taken in the analysis in regard to the following points: a) the structure assumed in the analysis, b) a correction for the non-nuclear scattering, and c) minor contributions of hydrogen terms.

a) In the calculation of the RD curve, the inner region ($q=0\sim15$) of the molecular intensity curve was spliced by a theoretical intensity curve $qM_c(q)$ computed with an assumed model*. The model listed in the first column A of Table II was assumed at the first stage; in this model all angles were assumed to be tetrahedral and the mean amplitudes calculated theoretically (see section V) were used**. The result of the first analysis was used to calculate the second RD curve, and as shown in the second B and the last column C of the table the second-stage parameters were made self-consistent with the final result of the analysis.

TABLE III. SELF-CONSISTENT ANALYSIS FOR THE FRACTIONS OF THE ISOMERS

Series		A	B	C	D
I	*trans*	100%	65%	67%	65%
II	〃	0%	48%	57%	61%

Besides the assumptions on the structural parameters, assumptions had to be made for the rotational isomers, i.e., the configurations and the fractions of the isomers[19]. It was found that the shape of the RD curve beyond 2.3Å is sensitive to these assumptions, though they had no appreciable effect on the inner part of the RD curve. A method of analysis similar to that used by Iwasaki[33] was applied as follows. The process is shown in Table III. Theoretical curves were calculated first for 100% *trans* form (azimuthal angle 180°) (Series I), and for 100% *gauche* form (azimuthal angle assumed to be 60°) (Series II). The frame structure was based on the model C of Table II. The area under the *trans* C-C peak in the resulting RD curve was compared with the theoretical value and the fraction of the *trans* form was estimated from the ratio (IB and IIB). A theoretical curve of the mixture of two isomers in this fraction was then spliced to the experimental curve and the same analysis was carried out. This procedure was repeated until a self-consistent result for

32) Y. Morino, K. Kuchitsu and M. Shibuya, Symposium on Structural Chemistry, Kyoto, Japan, Oct. 1958.

* The contribution of the theoretical molecular intensity curve spliced in the inner region ($q=0\sim15$) to the RD curve is such a slowly fluctuating function that slight changes in the parameters have no essential influences on either the peak positions or the peak widths, though there may be considerable changes in the peak areas. Account was taken of this point for estimating the errors.

** The hydrogen atoms in the methyl groups were assumed to be at the staggered configuration in euqilibrium with respect to the hydrogen and carbon atoms in the methylene groups. See L. G. Smith, *J. Chem. Phys.*, **17**, 179 (1949), Refs. 4 and 5 for ethane, Ref. 50 for ethyl chloride, and K. S. Pitzer, ibid., **12**, 310 (1944), for propane.

33) M. Iwasaki, S. Nagase and R. Kojima, This Bulletin, **30**, 230 (1957).

the fraction of the isomers was obtained (C and D). Since both series gave nearly the same values, the fraction of the *trans* form was thus found to be 60~65% in this analysis. The area under the *gauche* peak in the final RD curve was found to be about 35~40% of the theoretical maximum value (that is, the area which could be expected if the *gauche* form only were present), also in agreement with this result.

In conclusion, the model used for calculating the final RD curve was made sufficiently self-consistent, so that the result of the following RD analysis is essentially free from any arbitrary assumptions.

b) A correction for the non-nuclear scattering was made by using the method of Bartell[34]. A minor correction term $\Delta M(q)$ was subtracted from the observed molecular intensity $qM(q)$ to obtain $qM_c(q)$. The function $\Delta M(q)$, which is defined as

$$\Delta M(q) = qM(q) - qM_c(q)$$
$$= \sum_{i,j}{}' (c_{ij}/r_{ij})(\mu_{ij}-1)\exp(-l^2_{ij}s^2/2)\sin sr_{ij} \quad (3)$$

where

$$\mu_{ij} = c_{ij}/c_{ij}$$
$$c_{ij} = (Z_i - f_i)(Z_j - f_j)/\sum[(Z_i - f_i)^2 + S_i]$$

and

$$c_{ij} = Z_i Z_j/(\sum Z_i^2 + Z_i)$$

was calculated theoretically on the base of an assumed model. As in the former case a), the structure first assumed was that listed in the first column of Table II; and then ΔM was calculated again by using the second column of the same table. The elastic scattering factors for carbon and hydrogen atoms, $f(s)$, were taken from the tables of Viervoll and Ögrim[35], McWeeny[36], and Berghuis[37]. For the inelastic scattering factor of carbon, $S_C(s)$, Bewilogua's function[38] was used; as pointed out in his paper, this function which is based on the Thomas-Fermi model is still a good approximation for carbon. The S-function for hydrogen, $S_H(s)$, is approximated by $S_H(s) = 1 - [f_H(s)]^2$ after the argument of Mott and Massey[39]. In order to make the magnitude of the ΔM-function smaller, the value Z_H in Eq. 3 was put equal to 1.25. It seems probable that uncertainties in these factors have a negligible effect on the final result as compared with the experimental errors.

c) As there are many non-equivalent C–C, C–H and H–H distances in *n*-butane, (twenty-seven in the *trans* form, and thirty-five in the *gauche* form), thorough analysis of all distances is obviously too

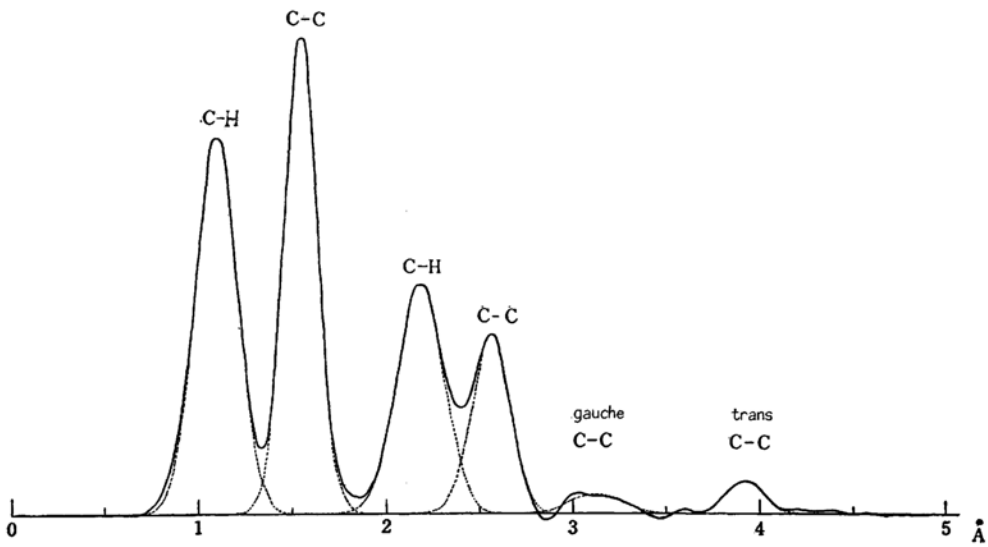

Fig. 3 Analysis of the average RD curve. The minor contribution illustrated in Fig. 2 is subtracted from the total curve. The dotted curves denote the best-fit Gaussian curves. The peaks represent (from left to right) the C–H, C–C, nonbonded C–H, nonbonded C–C, *gauche* C–C, and *trans* C–C distances, respectively.

34) L. S. Bartell, L. O. Brockway and R. H. Schwendeman, *J. Chem. Phys.*, **23**, 1854 (1955).
35) H. Viervoll and O. Ögrim, *Acta Cryst.*, **2**, 277 (1949).
36) R. McWeeny, ibid., **4**, 513 (1951).
37) J. Berghuis, et al., ibid., **8**, 478 (1955).
38) L. Bewilogua, *Physik. Z.*, **32**, 740 (1931).
39) N. F. Mott and H. S. W. Massey, "The Theory of Atomic Collisions", Oxford Univ. Press, London (1949).

complicated to be feasible. However, the structure of this molecule is principally determined by four main structure parameters, i.e., the C-H (average), C-C (average), C—H (average), and C—C distances. Since the contribution from these distances are exceedingly greater than that from the other distances, it is advantageous to subtract the minor contributions from the total RD, leaving the contributions from the principal parameters, which can then be analyzed uniquely. The minor contributions calculated by use of a self-consistent model are illustrated in Fig. 2 as a dotted line. The same procedure of obtaining such a self-consistent model as that discussed in a and b was undertaken. Tables II and III show that for the procedures a, b and c the model was simultaneously made self-consistent in two steps. The result is shown in Fig. 3.

Least-square Analysis of the Main Peak*.—The peak at 1.1Å in the RD curve (Fig. 3) corresponds to the C-H distance. The center of gravity which is equal to the mean distance was readily determined. The peak was found to be symmetrical with respect to the center, and accordingly, the curve could be fitted to a Gaussian function**.

The Gaussian function to be fitted is

$$y=y_0\exp(-Hx^2),\quad x=r-r_g \tag{4}$$

where r_g is the center of gravity. By taking the logarithm of both sides, the following linear equation is obtained.

$$Y=q-pX \tag{5}$$

where

$$X=x^2,\quad Y=\log_{10} y,\quad p=H\log_{10} e \quad \text{and} \quad q=\log_{10} y_0 \tag{6}$$

About ten sets of the observed values X_i's and Y_i's were used to determine the parameter p, under the condition that

$$\sum_i (\mathrm{d}y_i)^2=(\log_{10} e)^{-2}\sum_i y_i^2(\mathrm{d}Y_i)^2=\text{minimum} \tag{7}$$

Solving the equation for p,

$$p=\frac{[\sum y_i^2X_i]\,[\sum y_i^2Y_i]-[\sum y_i^2]\,[\sum y_i^2X_iY_i]}{[\sum y_i^2]\,[\sum y_i^2X_i^2]-[\sum y_i^2X_i]^2} \tag{8}$$

The parameter is related to the mean amplitude as

$$p=\log_{10} e/(4b+2l^2) \tag{9}$$

and

$$l=(\log_{10} e/2p-2b)^{1/2} \tag{10}$$

Since the standard error of the parameter p is given by

$$\sigma_p^2=\frac{[\sum y_i^2]}{[\sum y_i^2]\,[\sum y_i^2X_i^2]-[\sum y_i^2X_i]^2}\cdot\frac{\sum(\mathrm{d}y_i)^2}{n-2} \tag{11}$$

the standard error of the parameter l is readily obtained as*

$$\sigma_l=-\frac{\log_{10} e}{4lp^2}\sigma_p \tag{12}$$

The second peak at 1.54Å corresponds to the C-C distance. Because of the separation of 0.45Å between the C-H and C-C distances, a similar least-square analysis could be made with no ambiguity. The peaks for the non-bonded C-H and C-C distances are in a slightly closer separation. However, they were resolved by using the left side of the C-H peak, and the same procedure was applied. The results are listed in Table IV.

In the region beyond 3Å, two peaks

TABLE IV. RESULT OF THE LEAST-SQUARE ANALYSIS OF THE MRD CURVE

	$r_g(1)$[a]	Apparent mean amplitude	Area[b]
C-H (average)	1.092	0.084_6	0.987
C-C (average)	1.539	0.054_0	0.994
C-H (average)	2.179	0.103_2	0.970
C-C	2.553	0.074_8	1.060
C-C *trans*	3.914	0.069_6	0.590[c]

∠C-C-H (average) = 110°40′[d]

∠C-C-C = 112°6′

a) in Å unit

b) the ratio with respect to the theoretical absolute value

c) to be regarded as the fraction of the *trans* isomer

d) the value derived from $r_g(1)$ by Eq. 24

* The least-square analysis of RD curve has been reported recently by Bastiansen and Cyvin (O. Bastiansen and S. J. Cyvin, *Acta Chem. Scand.*, 11, 1789 (1957).). For a similar treatment of a $\sigma(r)$ curve, see the paper by Cruickshank et al. (D. W. J. Cruickshank and H. Viervoll, *Acta Chem. Scand.*, 3, 560 (1949).).

** The middle points of the curve at various peak heights were constant to a third decimal place of an angstrom. Strictly speaking, an $f(r)$ peak is expressed as

$$f(r)=\frac{c(\pi H)^{1/2}}{2r_e}\exp(-Hx^2)(1+ax+bx^2+cx^3+\cdots\cdots),\quad x=r-r_e$$

showing a slight distortion in trems of the parameters of anharmonicity and of the perpendicular amplitudes. However, the distortion is often so small that the curve can be interpreted as Gaussian. As will be shown later, the mean amplitude for $f(r)$ curve is almost the same as that for the probability distribution.

* The standard error is about 1%, being considerably smaller than the random errors estimated in section IV B.

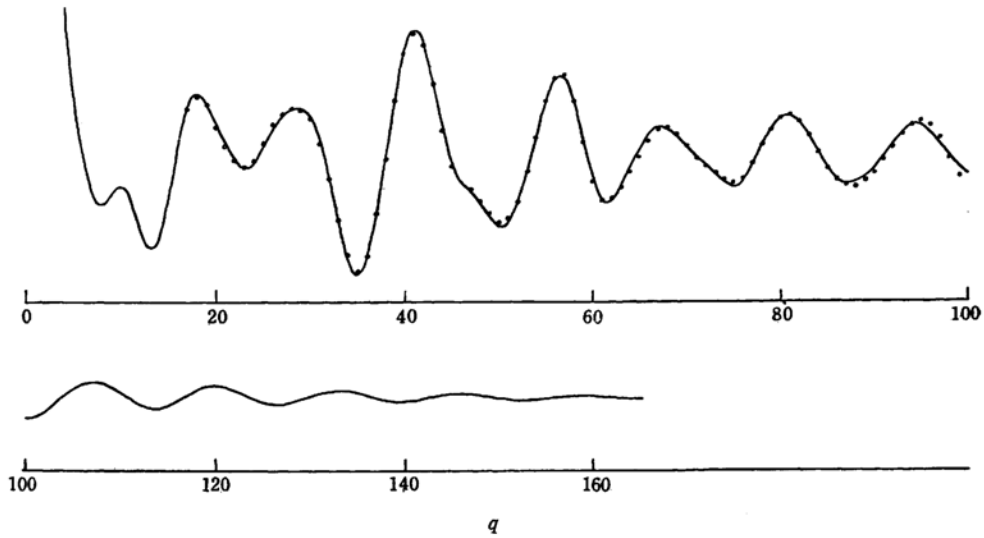

Fig. 4. Comparison of the observed and calculated molecular intensity curves. The solid line denotes the theoretical intensity calculated from the result of the MRD analysis (Table IV). The dots are the averaged experimental molecular intensity. These intensities fit within the experimental uncertainty illustrated in Fig. 1. The theoretical curve is extended beyond $q=100$, and is used in the UMRD analysis.
—— calculated ○ observed

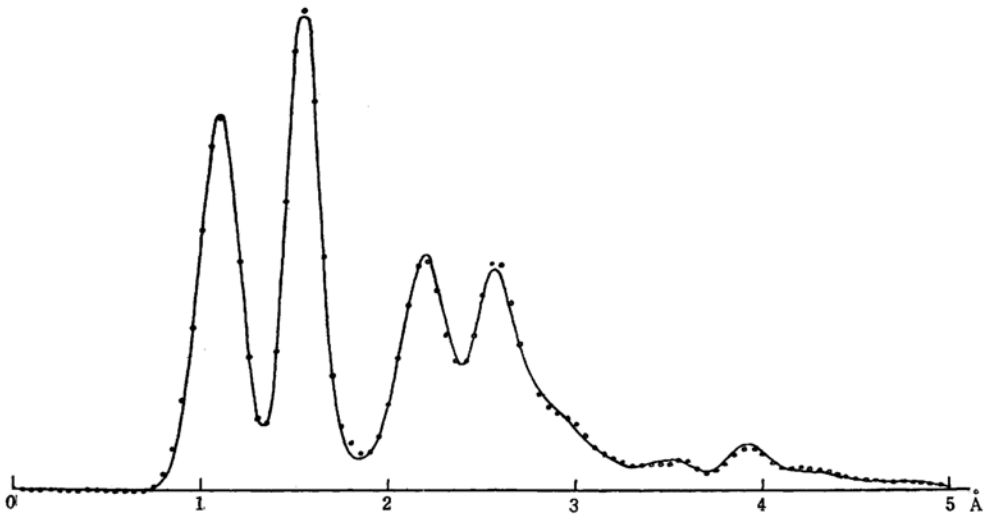

Fig. 5. Comparison of the observed and theoretical RD curves. The solid line represents the theoretical RD curve based on the result of the analysis assuming Gaussian distribution. The dots are the experimental MRD curve.
—— theoretical ○ observed (average)

appeared at 3.1Å and 3.9Å, corresponding to the *gauche* and the *trans* C–C distances, respectively. It affords a definite evidence for the rotational isomerism in this molecule. As the shape of the latter peak is practically Gaussian, the same procedure was applied, whereas only approximate values for the distance and its mean amplitude were estimated from the former peak. A theoretical intensity curve and an RD curve were calculated by the use of the result listed in Table IV. The agreement with the experimental curve is satisfactory, as shown in Figs. 4, 5 and Table V. The average index of resolution is about 99%.

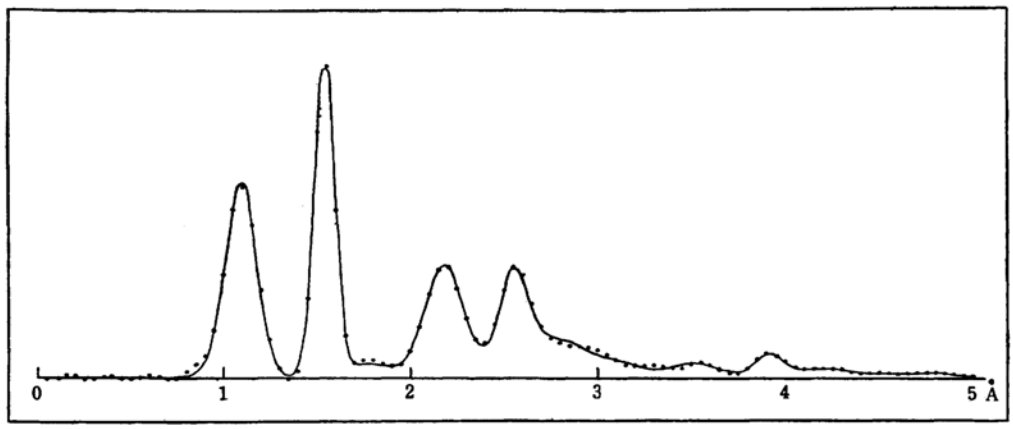

Fig. 6. Unmodified RD curve.
—— starting model (theoretical) ○ observed

TABLE V. COMPARISON OF THE OBSERVED AND THE CALCULATED INTENSITY CURVES

Max.	Min.	Peak position		Peak intensity	
		q_{calc}	q_{calc}/q_{obs}	I_{calc}	I_{obs}/I_{calc}
3		18.0	(0.990)	1.41	0.977
	3	23.1	1.004	−1.20	1.085
4		28.8	(1.022)	1.20	0.937
	4	34.9	0.995	−3.03	0.974
5		41.2	1.003	3.15	0.970
	5	50.0	0.996	−1.77	0.964
6		56.5	0.999	1.99	1.056
	6	61.4	1.001	−1.35	0.948
7		67.2	(0.991)	0.80	1.011
	7	75.3	1.002	−0.90	0.876
8		80.8	0.999	1.18	0.912
	8	87.2	0.996	−0.85	1.099
9		94.5	0.995	0.81	1.096
Average		—	0.998_8	—	0.993
Average Deviation		—	0.003	—	0.059

Unmodified Radial Distribution Curve.—By the same procedure as that described by Morino and Hirota[28], an unmodified radial distribution curve (UMRD), Eq. 13, was calculated for a further refinement of the analysis:

$$f(r)=\sum_{q=0}^{\infty}[w(q)qM_c(q)_{obs}+(1-w)qM_c(q)_{calc}]\times\sin\frac{\pi}{10}qr \qquad (13)$$

where $qM_c(q)_{obs}$ is the observed molecular intensity corrected for the non-nuclear scattering[34] and $qM_c(q)_{calc}$ is the calculated intensity based on the result of the analysis of the modified RD curve (Table IV and Fig. 4). The weight function $w(q)$ was so chosen that $w(q)\propto\exp[-c\Delta(q)^2]$, where $\Delta(q)$ is the amount of fluctuation among the observed intensity curves at a point q (Fig. 1), and c is a constant. The value $w(q)$ fluctuates somewhat irregularly with q between 100 and 80% for most of the experimental region (q=17~95), and is zero for the inner and outer parts. The UMRD curve is shown in Fig. 6. The analysis was carried out in the same way as that of the MRD curve (item 2). The results are given in Table VI and Fig. 6.

Estimation of the Errors in the Measurement of Interatomic Distances.—For the estimation of errors in the interatomic distances, sources of systematic errors in the scale factor and other errors in the observed RD curve must be considered. The main sources of systematic errors may be as follows.

a) The uncertainty in the scale-magnification ratio on the microphotometer trace, which is estimated to be about 0.1%.

b) The uncertainty in the camera length: it comes mainly from the difference between the position of the scattering center of the sample and that of the reference, and from the uncertainty in the position of the photographic plate. This error is about 0.1%.

c) The errors involved in the measurement of $L\lambda$: the product of the camera length L and the wavelength λ is determined by the measurement of the transmission pattern of gold foil. The standard error of the measurement is about 0.1%.

d) The drift of the wavelength: since a few minutes were required for exposure, the drift of the wavelength may be a cause of systematic error. In this experiment, however, the drift was controlled to within 0.05% by use of voltage stabilizers.

e) Errors in the determination of the

center in the photometric trace: they will cause error of less than 0.05%*. Assuming that these errors occur independently, a standard error in the scale factor is estimated to be about 0.2%.

f) A finite size of the light beam in the photometry: if the light beam has the rectangular shape of $a \times b$ on the photographic plate which is being measured (a being measured in the radial, and b in the perpendicular direction), the location of a halo of radius R on the plate suffers an inward shift of about $b^2/24R$. Since $a \times b = 0.1\,\text{mm.} \times 1\,\text{mm.}$ in this experiment, this shift has a uniform dependence on q, which is about 0.1% at $q=20$, and 0.01% at $q=60$. The correction was made for this effect though the magnitude is not important compared with other random errors.

For the standardization of the absolute scale factor, an analysis of carbon tetrachloride was made to check the apparatus and the method of analysis[39]. The C–Cl distance (the center of gravity of the $f(r)$ curve) was found to be 1.766Å, in good agreement with the results reported in the literature[34,40] within the experimental error.

Other errors were estimated from the variance of the results of the analyses for each of the five experimental RD curves, by using the standard statistical method on the assumption that this variance was caused by random errors. For the non-bonded peaks, possible sources of errors caused by the processes a, b and c stated in item 1 and the process of the decomposition of the composite peaks were also taken into account, the results of the above estimation are given in Table VI.

The Meaning of the Values Measured.— It is important to define clearly the meaning of the distances determined in this analysis, as pointed out by Bartell[41]. While the distance obtained above is the "center of gravity" or the "mean distance" of the $f(r)$ curve, it seems useful to correlate it to the $r_g(0)$ value, or the center of gravity of the probability distribution curve $P(r)$.

Including the anharmonicity in molecular vibrations[41] and the correction for the perpendicular amplitude, $P(r)$ may be expanded as (See f on page 756)

$$P(x) = (h/\pi)^{1/2} \exp(-hx^2) \times (1 + \alpha x + \beta x^2 + \gamma x^3 + \cdots\cdots) \tag{14}$$

where

$$x = r - r_e, \quad h = 1/2 < \Delta z^2 > \tag{15}$$

Then the mean value of the distance, $r_g(0)$, is expressed as

$$r_g(0) = \frac{\int_0^\infty r P(r)\,dr}{\int_0^\infty P(r)\,dr} = \frac{\int_{-\infty}^\infty (r_e + x) P(x)\,dx}{\int_{-\infty}^\infty P(x)\,dx}$$

$$= r_e + \alpha l^2 + \left(3\gamma - \frac{3}{2}\alpha\beta\right) l^4 + \cdots\cdots \tag{16}$$

where l^2 is the mean square amplitude, $< \Delta z^2 >$. On the other hand, the center of gravity of $f(r)$ is written by using the relation between $P(r)$ and $f(r)$,

$$f(r) = (\pi/16b)^{1/2} \int_{-\infty}^\infty [P(\rho)/\rho] \times \exp[-(r-\rho)^2/4b]\,d\rho \tag{17}$$

as

$$r_g(f) = \frac{\int_0^\infty r f(r)\,dr}{\int_0^\infty f(r)\,dr} = \frac{\int_0^\infty P(r)\,dr}{\int_0^\infty (P(r)/r)\,dr} \tag{18}$$

Therefore, it is equal to the center of gravity of the $P(r)/r$ curve, $r_g(1)$. By using Eq. 14, the difference between the above two is approximated by

$$r_g(0) - r_g(1) \cong \frac{l^2}{r_e} + \cdots\cdots \tag{19}$$

It amounts to a few thousandth of an angstrom; the second term is of the order of 10^{-5}Å. If a Morse-type potential function for the ground state of a diatomic molecule is assumed, as done by Bartell[41], the constants in Eq. 14 are in the following approximate relations,

$$\alpha = a, \quad \beta = 0, \quad \gamma = ah/3 \tag{20}$$

where a is a parameter of the Morse potential function, and Eqs. 16 and 19 agree with his expression (Eq. 4 of his paper). On the other hand, the center of gravity of the $rf(r)$ curve is given by

$$r_g(rf) = r_g(0) + 2b/r_g(1) \tag{21}$$

the difference being dependent on the damping factor b. The distance $r_g(0)$ can be obtained either from Eq. 19 or from 21. It is also obtained from the UMRD curve. The values of $r_g(0)$ obtained in this way are given in Table VI.

* The error due to an imperfect centering of the photographic plate during the scanning by the photometer is negligible, being of the order of a few ten thousandth of an angstrom, since the center was adjusted to within 5/100 mm. The error due to the deviation of the electron beam from the correct center of the sector during the exposure (which was within 5/100 mm.) is also negligible.

40) I. L. Karle and J. Karle, *J. Chem. Phys.* **17**, 1052 (1949).

41) L. S. Bartell, ibid., **23**, 1219 (1955).

TABLE VI. THE MEAN DISTANCES[a] AND ANGLES[b]

	MRD	UMRD	Standard error
C-H (average)	1.098	1.100	0.003
C-C (average)	1.540	1.539	0.003
C-H (nonbonded average)	2.182	2.181	0.005
C-C (nonbonded)	2.554	2.554	0.005
C-C (*gauche*)	3.12	3.13	0.02
C-C (*trans*)	3.913	3.911	0.009
∠C-C-H (average)	110°32′	110°22′	15′
∠C-C-C	112° 1′	112° 9′	9′

a) $r_g(0)$ in Å unit
b) the "mean angle" derived from $r_g(0)$ by Eq. 24

The mean square amplitude af a distance is defined by*

$$l^2(0)=\left[\int_0^\infty r^2P(r)\mathrm{d}r\right]\Big/\left[\int_0^\infty P(r)\mathrm{d}r\right]-[r_g(0)]^2 \tag{22}$$

whereas the mean square amplitude obtained from the radial distribution curve is

$$l^2(f)=\left[\int_0^\infty r^2f(r)\mathrm{d}r\right]\Big/\left[\int_0^\infty f(r)\mathrm{d}r\right]-[r_g(1)]^2 \tag{23}$$

A simple calculation using Eqs. 14 and 17 shows that the latter is equal to the mean square amplitude for the $P(r)/r$ curve, $l^2(1)$, plus $2b$, and the difference between $l^2(0)$ and $l^2(1)$ is only a minor correction as compared with the experimental error. (See f on page 756).

Determination of Valence Angles.—Following the above argument, the "mean angle" may be defined as the angle α derived by the following equation

$$\cos\alpha=(r_A^2+r_B^2-r_G^2)/(2r_Ar_B) \tag{24}$$

where r_A, r_B, and r_G are the mean values of the respective distances. The standard error of the angle is readily calculated to be

$$\sigma_\alpha=\left\{\left(\frac{1}{r_B}-\frac{\cos\alpha}{r_A}\right)^2\sigma_{r_A}^2+\left(\frac{1}{r_A}-\frac{\cos\alpha}{r_B}\right)^2\sigma_{r_B}^2+\left(\frac{r_G}{r_Ar_B}\right)^2\sigma_{r_G}^2\right\}^{1/2}\Big/\sin\alpha \tag{25}$$

The systematic error of the scale factor, 0.2%, is not included in σ_r's, because it has no effect on the angle. The result is given in Table VI.

Discussion Concerning the Longer Distances.—The *trans* C-C distance is calculated from the C-C distance $r_g(0)$ and the C-C-C angle assuming that the four carbon atoms are coplanar; it was found to be 3.926±0.003Å. On the other hand, the observed distance was 3.911±0.004Å*. The shortening, 0.015±0.005Å, can be interpreted as "significant", according to Cruickshank's definition[42]. It is likely that the shift is caused by a hindered rotation of the ethyl groups around the C-C axis taking the equilibrium position on the plane. The shift due to this effect was calculated theoretically by Karle and Hauptman[43]. It is calculated in a similar manner that the shift is 0.0120Å when the barrier V_0 is equal to 3.6 kcal./mol., and 0.0155Å when it is equal to 3.0 kcal./mol., in satisfactory agreement with the experimental shift. It is therefore inferred that the barrier height lies close to these values, in agreement with the value estimated by Pitzer, 3.6 kcal./mol.[14]

The azimuthal angle of the *gauche* form was calculated from the *gauche* C-C distance R_g(3.13±0.01Å) to be 67.5°±1.1°. The angle is thus nearly 60° as was usually assumed but possibly a little larger than that.

Estimation of Errors in the Mean Amplitude

The mean amplitudes listed in Table IV include both systematic and random errors. They were either corrected or estimated as shown in the following table.

A. Systematic errors
  Experimental
    a) effect of finite sample size: corrected,
    b) multiple or extraneous scattering: negligible,
    c) density-intensity calibration: estimated,
  Theoretical
    d) failure of Born approximation: corrected,
    e) effect of the possible difference in length between non-equivalent bonds: estimated,
    f) effect of perpendicular amplitude and of anharmonicity: negligible,
    g) effect of series termination: negligible,
    (in the case of MRD)
B. Random errors*

* The definition corresponds to u_a used by A. Reitan (Ref. 53).

* The error of the scale factor is not included in this comparison.

42) D. W. J. Cruickshank, *Acta Cryst.*, **2**, 65 (1949).

43) J. Karle and H. Hauptman, *J. Chem. Phys.*, **18**, 875 (1950).

* Errors which could not be treated as systematic errors were simply regarded as random errors though they might not be purely random in a strict sense.

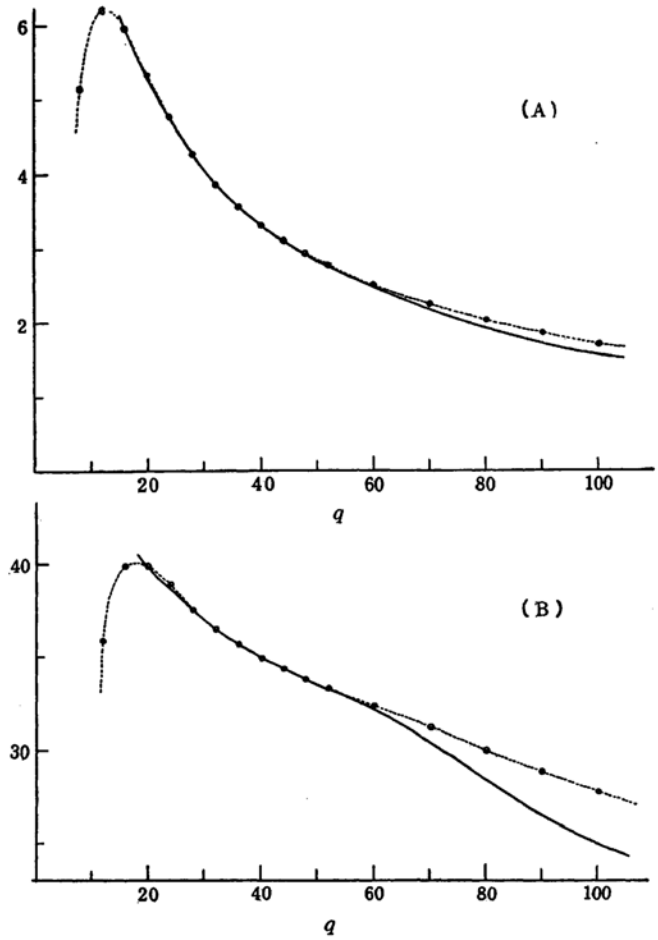

Fig. 7. Comparison of the background lines. Soild line: experimental; and dotted line: theoretical. The ordinate scales are adjusted in such a way that two curves coincide at $q=40$. (A) The background line obtained by use of an r^3-sector. (B) The curves shown in A are multiplied by $q^{1/2}$ to accentuate the difference; it amounts to about 10% at $q=100$.

Experimental: treated with a simple statistical method,
Computational: estimated.

These errors will be discussed as follows.

A. Systematic Errors.—*a) Effect of finite sample size.*—This effect was extensively studied by Karle[24], and also Harvey et al.[44] It is easily estimated if the distribution of the sample gas around the nozzle is known. The shape of the background line was found to be useful in this case for estimating the distribution. In Fig. 7 is shown a comparison of the observed background line with the calculated curve based upon the assumption that the diffracting molecules are located at an infinitesimal volume. The agreement is good in the inner region, whereas the deviation of the observed curve is clearly recognized beyond $q=60$. The nozzle used in this experiment is illustrated in Fig. 8. If this effect is attributed to the "screening" of the electrons at the nozzle edge, the distribution is estimated with the following simple assumptions:

1) The decrease in the observed background compared with the theoretical background is essentially caused by process in which a small fraction of the electrons scattered by the sample hit the wall of nozzle and do not reach the photographic plate (Fig. 8).

2) Since the beam diameter is much less than the nozzle aperture, a one-dimensional distribution of the sample gas, the area being normalized, is considered. Then the decrease is determined by the area of the shadowed region in Fig. 8.

44) R. B. Harvey, F. A. Keidel and S. H. Bauer, *J. Appl. Phys.*, **21**, 860 (1950).

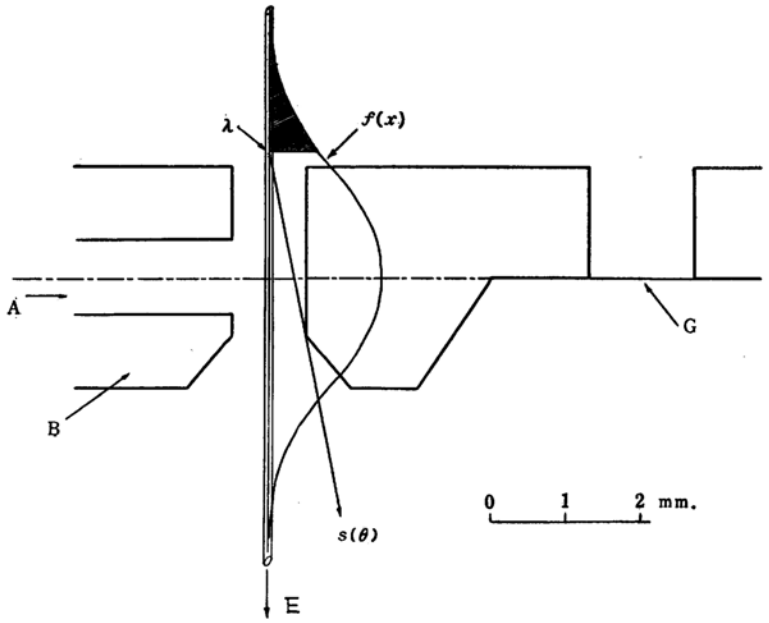

Fig. 8. "Screening effect" of the nozzle. An enlarged cross section of the drum-type nozzle is illustrated. A: gas inlet; B: nozzle body; E: electron beam (the cylinder represents a rough measure of the diameter); $f(x)$: normalized one-dimensional distribution of the gas; G: gold foil used as the reference. It is assumed that the electrons scattered at the point farther than the critical point $\lambda(\theta)$ (shaded region) in the direction of $s(\theta)$ are completely screened by the wall of the nozzle and do not reach the photographic plate, and that the scattered intensity undergoes a fractional decrease proportional to the shaded area.

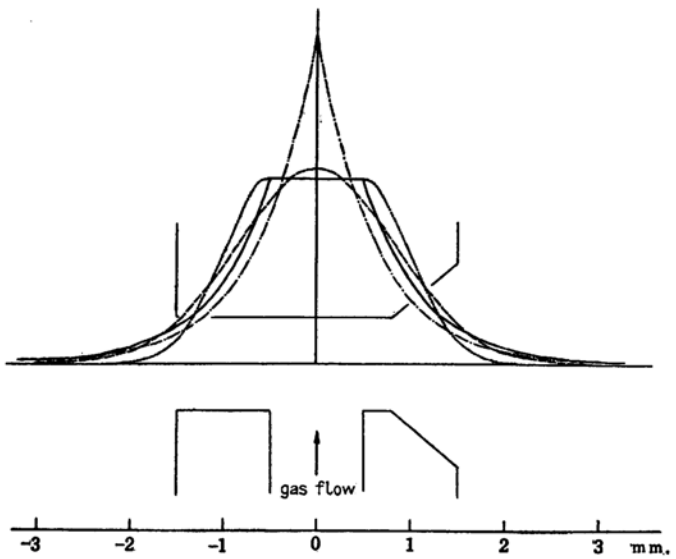

Fig. 9. Distribution functions of the gas spreading. It is assumed that they are symmetrical across the center of the nozzle inlet, and the areas are normalized. Solid line : flat and exponential; dotted line: flat and Gaussian; chain line: exponential; and broken line: Gaussian. It is seen that the distributions are all practically zero outside the nozzle.

3) The distribution is symmetrical across the center of the nozzle inlet.

In additon to these assumptions, the following simple analytical functions were assumed for the distribution, and parameters were determined to reproduce the experimental fractional decrease. The shapes of the distribution functions assumed are:

Exponential:

$$f(x)=\frac{1}{2}\rho\exp(-\rho|x|),\quad \rho=1.593 \tag{26}$$

Gaussian:

$$f(x)=(\sigma/\pi)^{1/2}\exp(-\sigma x^2),\quad \sigma=0.700 \tag{27}$$

Flat and exponential:

$$f(x)=c,\quad |x|\leq x_0,\quad c=0.45$$
$$f(x)=c\exp(-\alpha|x|),\quad |x|>x_0,\quad \alpha=1.636 \tag{28}$$

and Flat and Gaussian:

$$f(x)=c,\quad |x|\leq x_0,\quad c=0.45$$
$$f(x)=c\exp(-\beta x^2),\quad |x|>x_0,\quad \beta=2.103 \tag{29}$$

where x is the distance in millimeters measured from the center of the nozzle inlet, and $x_0=0.5$ mm. is the radius of the inlet. The distribution is illustrated in Fig. 9. It is seen that the density is practically zero outside the nozzle, though the localization is somewhat poorer than that of Karles' nozzle estimated in their paper[24].

The distribution function being assumed, the damping of the molecular intensity (a contribution of a particular atomic pair whose equilibrium distance is r) caused by the spreading of the sample is calculated by the following integration:

$$M=\int_{-\infty}^{\infty}M(s)f(x)\mathrm{d}x=\int_{-\infty}^{\infty}(\text{const.})\times\exp\left(-\frac{l^2}{2}s^2\right)\frac{\sin sr}{sr}f(x)\mathrm{d}x \tag{30}$$

where s is a function of the camera length L, which is the sum of L_0+x, L_0 being the camera length referred to the nozzle center. This may be expressed as:

$$s(x)=\frac{2\pi R}{\lambda}\frac{1}{(L_0+x)}\left[1-\frac{3}{8}\frac{R^2}{(L_0+x)^2}\right]$$
$$=\frac{2\pi R}{\lambda L_0}\left(1-\frac{3R^2}{8L_0^2}\right)\left(1-\gamma\frac{x}{L_0}\right) \tag{31}$$
$$=s_0\left(1-\gamma\frac{x}{L_0}\right)$$

$$\gamma=1-\frac{3R^2}{4L_0^2}\sim 1-7\times10^{-5}s_0^2 \tag{32}$$

where R is the radius on the photographic plate. Substituting Eq. 31 into 30 and remembering that $f(x)$ is assumed to be a symmetrical function of x, Eq. 30 is transformed into Eq. 33 giving the damping of the molecular intensity:

$$M/M_0=\int_{-\infty}^{\infty}f(x)\cos\alpha x\mathrm{d}x,\quad \alpha=\gamma s_0 r/L_0 \tag{33}$$

where $M_0(s_0)$ refers to L_0 (the molecular intensity scattered by a point source).

TABLE VII. CORRECTION AND ESTIMATION OF ERRORS IN THE MEAN AMPLITUDES

		$C-H_{av}$	$C-C_{av}$	$C-H_{av}$	C-C	$C-C_{trans}$
Systematic errors (%)						
(a) Finite sample size	cor	+0.5	+2.1	+1.0	+3.0	+7.2
(b) Multiple or extraneous scattering	neg	—	—	—	—	—
(c) *D-E* calibration[a]	est	$<\pm3$	$<\pm5$	$<\pm4$	$<\pm3$	$<\pm3$
(d) Born approximation	cor	+2.3	—	+1.6	—	—
(e) Non-equivalent bonds	est	$<+0.2$	$<+1.6$	$<+0.4$		
(f) Perpendicular amplitude and anharmonicity	neg	—	—	—	—	—
(g) Series termination (in the case of MRD)	neg	—	+0.7	—	—	—
Random errors (%)	est	$\sim\pm4$	$\sim\pm3.5$	$\sim\pm4$	$\sim\pm8$	$\sim\pm7$
Total standard errors[b] (%)	est	$\sim\pm5$	$\sim\pm5$	$\sim\pm5$	$\sim\pm9$	$\sim\pm9$
Apparent mean amplitude (UMRD)		0.085_5	0.053_7	0.100_1	0.080_0	0.072_9
Corrected mean amplitude (A)		0.083_1	0.052_6	0.097_5	0.077_6	0.067_7
Standard error (A)		0.004	0.003	0.005	0.007	0.007

cor: corrected; est: estimated; neg: negligible

a) The meaning of the symbol $<\pm$ is that the sign may be positive or negative, but that the absolute value should not exceed the given figure.

b) The uncertainties involved in the corrections a and d are estimated to be $\pm70\%$ of the correction values.

On calculating the damping function (Eq. 33) analytically using Eq. 26 through 29 for $f(x)$*, it was found that all assumed distributions give nearly the same result, and it can be expressed in a good approximation in the form

$$M/M_0=\exp(-\varepsilon s^2) \tag{34}$$

An apparent increase in the mean amplitude is accordingly given by

$$(l+\Delta l)^2=l^2+2\varepsilon, \quad \Delta l\sim\varepsilon/l \tag{35}$$

The percentage correction for each interatomic distance is given in Table VII. It should be noted that the parameter ε is a function of r, and that the correction is greater for the longer distance, and for the harder distance (i.e., the distance which has a smaller mean amplitude), as already pointed out[24,44].

b) Effect of multiple or extraneous scattering.—This effect was considered to be negligible in view of the following argument.

1) No appreciable extraneous scattering was found to be present, as stated in the experiment part.

2) Care was taken in the experiment to reduce the sample pressure during the exposure[25]; the flow rate was sufficiently "slow" in the sense discussed by Harvey et at.[44] to avoid the multiple scattering.

3) The observed background line agrees well with the theoretical form, showing no appreciable multiple scattering present (Fig. 7).

4) The index of resolution is nearly unity, which affords another point of support.

5) It was shown by Karle[24] theoretically that even if a considerable amount of multiple scattering were present, it would raise the background uniformly and decrease the molecular intensity also in a uniform manner. Consequently it does not change the damping factor of the molecular term significantly.

c) Uncertainty in the density-intensity calibration curve. — This effect may be estimated in the following way. Suppose the calibration function $E(D)$, in which E and D denote the intensity and density, respectively, is obtained experimentally instead of the true function $E^0(D)$ which is unknown. Since the functions E^0 and E are both uniform functions of D, their ratio may be expanded as

$$E(D)/E^0(D)=c(1+\alpha D+\beta D^2+\cdots\cdots) \tag{36}$$

If the maximum or the minimum point of the intensity curve and the background intensity of the same point are denoted by E_1 and E_2 respectively, and the densities which correspond to E_1 and E_2 on the $D-E$ curve by D_1 and D_2, the fractional error R in the molecular intensity obtained from Eq. 1 is given by

$$\begin{aligned} R&=\left\{\frac{E_1^0(1+\alpha D_1+\beta D_1^2)}{E_2^0(1+\alpha D_2+\beta D_2^2)}-1\right\}\Big/\left\{\frac{E_1^0}{E_2^0}-1\right\} \\ &=1+\frac{E_1^0}{E_1^0-E_2^0}\{\alpha(D_1-D_2) \\ &\quad+(2\beta-\alpha^2)D_2(D_1-D_2)\} \end{aligned} \tag{37}$$

Since D is nearly proportional to E,

$$R\sim1+\alpha D_1+(2\beta-\alpha^2)D_1D_2 \tag{38}$$

On the other hand, the experimental measure of the uncertainty in the $D-E$ curve may be estimated 1) by the variance of the slope of the observed background lines, and 2) by the difference between the $D-E$ curve obtained by Karles' method and that obtained by Bartell's method using the same density curves.

It was found that the magnitude of the parameters α or β is about ±0.05. Since the maximum density in this experiment was about 0.8, the upper limit of the error in the molecular intensity was estimated to be 10%. Possible error in the mean amplitude caused by this effect is accordingly estimated for each distance by fitting roughly to an exponential function, and listed in Table VII.

d) Failure of Born approximation. — It is well known that the theoretical expression 4 for the scattering of electrons by molecules is derived by Born approximation, which is not always justified[39]. The failure of Born approximation was first pointed out by Schomaker and Glauber[45,46], and discussed by Hoerni and Ibers[47]. The effect on the mean amplitude, an apparent increase, was discussed by Bartell and

* For example, the use of Eq. 26 gives

$$M/M_0=\rho^2/(\alpha^2+\rho^2)$$

and the use of Eq. 27 gives

$$M/M_0=\exp[-\alpha^2/(4\sigma)]$$

The latter formula corresponds to Eq. 13 of Karles' paper[24]. More strictly, the upper limit of the integral 30 should be the cut-off point, λ, shown in Fig. 8, which is a function of s. A detailed calculation shows, however, that the molecular term assumes an additional factor and a phase shift which are both of a negligible order of magnitude.

45) V. Schomaker and R. Glauber, *Nature*, **170**, 291 (1952).

46) R. Glauber and V. Schomaker, *Phys. Rev.*, **89**, 667 (1953).

47) J. A. Hoerni and J. A. Ibers, ibid., **91**, 1182 (1953).

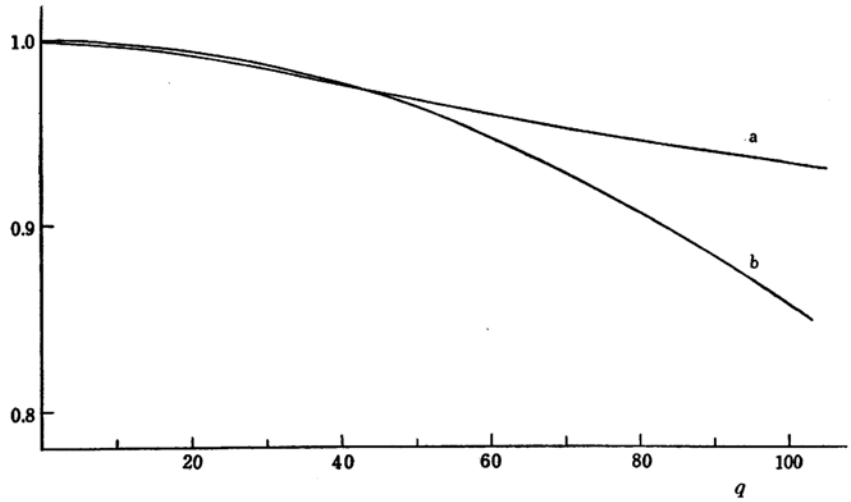

Fig. 10. Approximation of the phase shift $\cos \Delta\eta$ by an exponential function. a) $\cos \Delta\eta$ for the C-H pair; and b) $\exp(-\delta s^2/2)$ where $\delta = 3.096 \times 10^{-4}$. The deviation is about 7% at $q = 100$.

Brockway[48,34]. In the following a similar correction for this effect is carried out.

The expression is given by

$$sM(s) = \sum_{i,j}{}' (c_{ij}/r_{ij}) \exp\left(-\frac{l_{ij}^2}{2} s^2\right) \times \cos \Delta\eta_{ij} \sin sr_{ij} \quad (39)$$

$$\Delta\eta_{ij} = \eta_i(s) - \eta_j(s) \quad (40)$$

The C-H pairs are the only objects to be considered for this molecule, since the phase shift $\Delta\eta$ appears only for a pair of different atoms. The phase function $\eta(s)$ was calculated and tabulated by Ibers and Hoerni[49]. Since the values are based on the Thomas-Fermi model, they may naturally be a poor approximation for carbon and hydrogen. According to their argument[49], however, the phase shift $\Delta\eta$ is probably reliable, and in addition, the magnitude of η for hydrogen is very small. The Eq. 13 of their paper is available to convert the values to η for the accellerating voltage used in this experiment.

The damping function $\cos \Delta\eta_{C-H}$ was approximated by an exponential form, as discussed by Bartell,

$$\cos \Delta\eta_{C-H}(s) \sim \exp(-\delta s^2/2) \quad (41)$$

the value δ being derived numerically in the following average, taking the damping function (including the artificial temperature factor) as a weight $w(s)$

$$\int w(s) [\cos \Delta\eta - \exp(-\delta s^2/2)] \, ds = 0 \quad (42)$$

$$w(s) = \exp\left(-\frac{l^2_{C-H}}{2} s^2\right) \exp(-bs^2) \quad (43)$$

The value thus obtained is

$$\delta = 3.096 \times 10^{-4} \text{ Å}^2 \text{ for bonded C-H,}$$

and $\delta' = 3.431 \times 10^{-4}$ Å^2 for non-bonded C-H.

The maximum deviations of the exponential functions from the cosine functions were about 7% (Fig. 10). These deviations were further corrected by introducing a δM-function in a way similar to that discussed in the case of non-nuclear scattering[34],

$$\delta M(s) = M_{C-H}(s)\{1 - \cos \Delta\eta/\exp(-\delta s^2/2)\} + M'_{C-H}(s)\{1 - \cos \Delta\eta/\exp(-\delta' s^2/2)\} \quad (44)$$

The order of magnitude of this function is less than 1% of the molecular intensity, and therefore it barely contributes to the RD curve.

The percentage correction for this effect to the mean amplitude is given in Table VII.

e) Effect of the possible difference in the distances between non-equivalent bonds. — It should be noted that the C-H, C-H (non-bonded), and C-C distances observed are the average values of the two respective non-eqivalent distances, i.e., C-H (methyl) and C-H (methylene), and C-C (end) C-C (central). Should these distances differ slightly, as may be the case, observed mean amplitudes will show apparent increase.

This effect is readily treated as follows. Suppose there are two Gaussian peaks 1 and 2 (peak positions r_1 and r_2, and peak

48) L. S. Bartell and L. O. Brockway, *Nature*, 171, 978 (1953).
49) J. A. Ibers and J. A. Hoerni, *Acta Cryst.*, 7, 405 (1954).

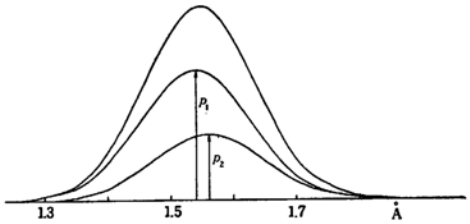

Fig. 11. A composite peak of non-equivalent C-C distances. The peak is slightly broader than each of the component peaks.

heights p_1 and p_2, respectively) close together (Fig. 11). Their mean amplitudes are assumed to be the same, l. The composite peak will then be given by

$$P=p_1\exp\{-H(r-r_1)^2\}+p_2\exp\{-H(r-r_2)^2\} \quad (45)$$
$$H=(2l^2+4b)^{-1}$$

If the origin of the distance r is chosen at the center of gravity, the composite peak is expresed as

$$P=\exp(-Hr^2)\left[\sum P_i\exp(2Hr_ir)\right] \quad (46)$$
$$P_i=p_i\exp(-Hr_i^2), \qquad i=1,2 \quad (47)$$

The term in the bracket being expanded,

$$\sum_{1,2} P_i\exp(2Hr_ir) = (P_1+P_2)+2H^2rp_1r_1(r_1^2-r_2^2) + 2H^2r^2(P_1r_1^2+P_2r_2^2) \quad (48)$$

The second term is about a small percentage of the third term and does not affect the width. Therefore, the peak is expressed as a Gaussian function to a good approximation:

$$P=(P_1+P_2)\exp(-H'r^2) \quad (49)$$

where

$$H'=H-2H^2(P_1r_1^2+P_2r_2^2)/(P_1+P_2) \quad (50)$$

The coefficient H is related to l in Eq. 45, so that the apparent increase in l is calculated by Eq. 50.

The splittings of the distances are definitely too small to be detected in this experiment; the only available references seem to be the splitting of the C-H distances in ethyl chloride estimated in the microwave spectroscopy[50],

C-H(methyl) = 1.110Å

C-H(methylene) = 1.101Å

and the plausible values predicted by Glockler from the consideration of bond-energy data[51],

C-H(methyl) = 1.097Å

C-H(methylene) = 1.0985Å

C-C(end) = 1.559Å

C-C(central) = 1.564Å (in *n*-butane)

The maximum possible percentage apparent increases listed in Table VII are calculated by inserting in Eq. 50 the value:

r_1-r_2(C-H bonded) = 0.01Å

r_1-r_2(C-H non-bonded) = 0.02Å

and r_1-r_2(C-C bonded) = 0.02Å

It is seen that this effcet is possibly negligible.

f) The effect of perpendicular amplitude and of anharmonicity. — The probability distribution function of an interatomic distance including both parallel and perpendicular amplitudes was derived by Morino and Hirota[52]

$$P(r)=(h/\pi)^{1/2}\exp(-hx^2)\times(1+c_1x+c_3x^3+\cdots\cdots) \quad (51)$$

where

$$h=1/2<\Delta z^2>, \qquad x=r-r_e$$

and

$$c_1=(h/r_e)\left[<\Delta x^2>+<\Delta y^2>-6h(<\Delta z\Delta x>^2+<\Delta z\Delta y>^2)\right] \quad (52)$$
$$c_3=(4h^3/r_e)\left[<\Delta z\Delta x>^2+<\Delta z\Delta y>^2\right] \quad (53)$$

On the other hand, the following $P(r)$-function including anharmonic vibration was given by Bartell[41] and by Reitan[53].

$$P_{anh}(r)=(h/\pi)^{1/2}\exp(-hx^2)\times(1+a_1x+a_2x^2+a_3x^3+\cdots\cdots) \quad (54)$$

Since these effects introduce only slight modifications on the Gaussian distribution, the combined effect may be written in the first approximation,

$$P(x)=(h/\pi)^{1/2}\exp(-hx^2)(1+c_1x+c_3x^3)\times(1+a_1x+a_2x^2+a_3x^3) \quad (55)$$
$$=(h/\pi)^{1/2}\exp(-hx^2)\times(1+\alpha x+\beta x^2+\gamma x^3+\cdots\cdots) \quad (14)$$

The mean square amplitude for this distribution is readily calculated as

$$l^2(0)=<\Delta z^2>+\left(2\beta-\frac{3}{2}\alpha^2\right)(<\Delta z^2>)^2 \quad (56)$$

$l^2(0)$ can be obtained from $l^2(f)$ by the equation,

50) R. S. Wagner and B. P. Dailey, *J. Chem. Phys.*, **23**, 1355 (1955).
51) G. Glockler, ibid., **17**, 747 (1949).
52) Y. Morino and E. Hirota, ibid., **23**, 737 (1955).
53) A. Reitan, *Acta Chem. Scand.*, **12**, 131, 785 (1958).

$$l^2(0)=l^2(f)-2b+\left[\frac{1}{2}\alpha^2+\frac{3\alpha}{2r_e}-3\alpha\beta r_e+4\beta+4\beta^2 r_e^2-\frac{1}{r_e^2}\right]l^4+\cdots\cdots \quad (57)$$

It is to be noted that a minor fractional correction is of the order of $l^2/2r_e^2$, which is less than 0.5%. Thus the effect of anharmonicity or the perpendicular amplitude are regarded as negligible, at least in obtaining the mean amplitude defined in Eq. 56.

Care should be taken, however, in the comparison of the amplitudes observed in this way with that calculated from the vibrational data. For the influence of anharmonicity on the mean amplitudes, interesting discussions were made by Reitan[53]. According to his calculation, apparent mean amplitudes of O–H and H–H bonds in water molecule based on the harmonic approximation are about 5% smaller than those which include the anharmonic effect. For heavier molecules such as Br_2, the correction was shown to be negligible.

g) Effect of series termination. — The MRD function was computed by use of Eq. 2 taking the upper limit of the integral as q_{max} instead of infinity. According to Waser and Schomaker[54], an exponential damping function $\exp(-bs^2)$ was adopted in the present analysis for the modification of the RD, the factor b being chosen following the usual convention that $\exp(-bs_{max}^2)=0.1$.

Since the intensity curve multiplied by the damping factor is given by a sum of the contribution of the component terms,

$$sM(s)=\sum_n sM_n(s)=\sum_n (c_n/r_n)\times\exp(-s^2/4H_n)\sin sr_n \quad (58)$$

the Fourier inversion is also expressed as a sum,

$$f(r)=\sum_n\int_0^\infty sM_n(s)\sin sr\,ds-\sum_n\int_{s_{max}}^\infty sM_n(s)\sin sr\,ds=f_0(r)-f'(r) \quad (59)$$

The RD function actually obtained is the sum of $f_0(r)$, the true RD function, and $-f'(r)$, additional ripples. Taking out the n-th contribution to $f'(r)$, and using Eq. 58, $f'_n(r)$ is given by

$$f'_n(r)=(c_n/2r_n)\left\{\int_{s_{max}}^\infty \cos s(r_n-r)\times\exp(-s^2/4H_n)ds-\int_{s_{max}}^\infty \cos s(r_n+r)\exp(-s^2/4H_n)ds\right\} \quad (60)$$

where the second term is usually negligible. At the center of the RD peak, i.e., $r=r_n$, the function $f'_n(r)$ has its maximum value, which is expressed in terms of the error integral, $\Phi(s_{max}/\sqrt{2H_n})$. Elsewhere, $f'_n(r)$ reveals itself as a ripple of the period of slightly less than $2\pi/s_{max}$. It is obviously symmetrical across the center of the peak and damps slowly as $|r-r_n|$ increases.

In the present example, $s_{max}=10\pi$, $H_n\sim66$ for the C–C bond which has the smallest damping factor, and $H_n\sim50-30$ for the other bonds. By the evaluation of the error integral, it was found that the maximum magnitude of f'_n is about 0.6% of the peak height for the C–C peak, and less than 0.1% for the others. The effect is thus unquestionable except for the C–C peak, and even in that case, it causes a slight symmetrical distortion of the C–C peak itself and an apparent increase of about 0.7% in its mean amplitude. A shift of the distance r_g of the adjacent peaks due to this effect amounts to only a few ten thousandth of an angstrom.

A similar, but more extensive discussion was carried out by Morimoto in his recent RD analysis of evaporated crystallites[55]. The result is in agreement with the estimation described above.

B. Random Errors.—The main origins of experimental random errors are 1) errors introduced in the photographic process (exposure, development, etc.), 2) errors of the microphotometry, 3) errors of the measurement of the photometer curve, and 4) errors introduced in the failure of drawing a proper background line, etc.

These errors are included in the molecular intensity and, being Fourier inverted, reveal themselves as random fluctuations or "ghosts" in the RD curve, which cause errors in the measurement of mean amplitudes.

The following features may be used as the measures of these fluctuations.

1) Fluctuations of the baseline in the regions where no interatomic distance should exist: as shown previously, there are no appreciable fluctuations in the baseline from 0 through 0.7Å (Fig. 3). Beyond 2.8Å of the RD curve, however, there

54) J. Waser and V. Schomaker, *Revs. Modern Phys.*, **25**, 671 (1953).

55) H. Morimoto, *J. Phys. Soc. Japan*, **13**, 1015 (1958).

appear small fluctuations, which probably come from the experimental errors together with the computational errors.

2) Difference among RD curves illustrated in Fig. 2, obtained by the independent procedure: the maximum deviation amounts to a small percentage of the peak height.

3) The standard errors given in the least-square analysis of the mean RD curve (Eq. 12): they were found to be about 1% of the mean amplitudes.

4) Deviations of the areas of the RD peaks from the theoretical values: the ratios listed in Table IV show that the deviations amount to a small percentage.

In order to estimate the random errors in the mean amplitudes, it seems possible to make use of one of the following methods:

1) Use of the variance in the results of the least-square analysis of the individual RD curves, which may correspond to the "mean square deviation between classes",

2) Use of the square sum of the residuals in the process 1, which may correspond to the "mean square deviation within classes",

3) Use of the difference among the RD curves to estimate the standard error at each point of the peak.

Each method was used in the present estimation together with Eqs. 11 and 12. Errors introduced in the computational process were also taken into account. Important ones among them would be 1) errors in the computation (rounding-up errors, etc.), 2) improper assumptions used in the analysis (structure, scattering factors, etc.), 3) ambiguity in the decomposition of the composite peak, and 4) improper correction for various systematic errors. A plausible estimation was made utilizing the experience in the self-consistent analysis described above. As for the effect 4, the corrections for systematic errors were considered to include ±70% uncertainties.

The results of the estimation of random errors are listed in Table VII. In the last row of the table are listed the mean amplitudes for which suitable corrections have been made, with their total standard errors which include all errors estimated in the above consideration.

Calculation of the Mean Amplitudes

In order to correlate the observed mean amplitudes to be spectroscopic data, a calculation of the mean amplitudes was carried out. Because of the lack of knowledge of the force constants, a simple and approximate treatment was made.

First the skeleton vibrations were considered by assuming a methyl or a methylene group as a particle for the *trans* and the *gauche* forms. The Wilson's G and F matrices for the *trans* form given as follows[56,58].

$$\begin{array}{lll} & \mathbf{G} & \mathbf{F} \\ \mathrm{A}: & \begin{bmatrix} 2\mu_0 & & \\ 2\mu_0\cos\varphi & \mu_0+\mu & \\ -\sqrt{2}\,\rho_0\mu_0\sin\varphi & -2\rho_1\mu_0\sin\varphi & \rho_0^2(\mu_0+\mu)+4\mu_0(\rho_1^2-\cos\varphi) \end{bmatrix} & \begin{bmatrix} K_0+2a_0F & & \\ \sqrt{2}\,cF & K_1+a_1F & \\ \sqrt{2}\,\rho_1 d_0F & \rho_0 d_1F & H+bF \end{bmatrix} \\ \mathrm{B}: & \begin{bmatrix} \mu_0+\mu & \\ 0 & \rho_0^2(\mu_0+\mu) \end{bmatrix} & \begin{bmatrix} K_1+a_1F & \\ \rho_0 d_1F & H+bF \end{bmatrix} \end{array} \tag{61}$$

TABLE VIII. COMPARISON OF THE NORMAL FREQUENCIES FOR THE TRANS FORM

		Skeleton vibration	Observed (cm^{-1})			Calculated (cm^{-1})	
			a	b	c	A set	B set
A_g	ν_1	stretching	1059	1058	1056	1075	1068
	ν_2	mixed	837	835	833	835	909
	ν_3	deformation	425	432	(319?)	432	374
B_u	ν_4	stretching	—	970?	956.4	955	993
	ν_5	deformation	—	?	215.0	295	277

a: Ref. 60, b: Ref. 11, c: Refs. 9 and 15.

56) E. B. Wilson, Jr., *J. Chem. Phys.*, **7**, 1047 (1939); **9**, 76 (1941).

57) E. B. Wilson, Jr., J. C. Decius, and P. C. Cross, "Molecular Vibrations" McGraw-Hill, New York (1955).

TABLE IX. CALCULATED VALUES FOR THE MEAN AMPLITUDES (skeleton) (in Å unit)

Atomic pair	Observed (UMRD)	Calculated			
		trans Form		*gauche* Form	
		A set	B set	A set	B set
C-C (CH_2-CH_2)	$0.052_6\pm0.003$	0.048_7	0.049_8	0.049_1	0.049_9
C-C (CH_2-CH_3)		0.051_6	0.048_9	0.051_3	0.049_0
C-C (nonbonded)	$0.077_6\pm0.007$	0.069_2	0.079_4	0.068_2	0.078_2
C-C (*gauche*)	0.136	—	—	0.161_1	0.169_1
C-C (*trans*)	$0.067_7\pm0.007$	0.070_4	0.079_2	—	—

where the symbols have their usual meaning[57,59]. Two different sets of Urey-Bradly force constants were taken. One set A is that given by Shimanouchi[60], which was selected to the fit to Raman spectra of *n*-butane,

$K_0=4.0$, $K_1=3.2$, $H=0.11$, $F=0.96$ and $F'=0$

The other set B is that reported as the force constants of methyl and methylene groups[59], and taken by Hayashi in his calculation of the normal vibration of *n*-pentane molecule as a five-body problem[61].

$$K_0=3.7,\quad K_1=4.0,\quad H=0.20,\quad F=0.33$$
$$\text{and } F'=-0.1F$$

These force constants being inserted in Eq. 61, it is an easy and straightforward computation to obtain the normal frequencies[56,57] and the mean amplitudes[62,63]. A comparison of the frequencies for the *trans* form is given in Table VIII. The assignment of the skeleton frequencies was made by several authors[11,15,60,64], and there seems to be no difficulty except in the lowest B_u (bending) mode*. Although the band 215.0 cm^{-1} observed in the far infrared spectra was assigned to this mode by Gates, and no other band was found between 400 and 170 cm^{-1}, it seems likely that this mode has a little higher frequency. The agreemment of the calculated frequencies with the observed is much better for the A-set. Accordingly, the mean amplitudes calculated with the A-set may be the more reliable.

For the mean amplitudes of the *gauche* form the barrier against the torsional motion was assumed to be 3.6 kcal./mol.[14] An approximate method[63] was applied. These results are shown in Table IX. The larger amplitude obtained for the *gauche* C–C distance as compared with the *trans* C–C is just as expected.

For the mean amplitudes of the distances including hydrogen atoms, methyl groups were approximated by chlorine atoms, that is, the mean amplitudes of the H–H and C–H atom pairs in 1,2-dichloroethane were calculated, be cause the L matrices for this molecule calculated by Nakagawa[65] were available. Although this approximation apparently seems drastic, past experience on the calculation of mean amplitudes assures that it will give sufficiently correct values for this purpose[63]. The results obtained are listed in Table X. The mean amplitude of the C–C distance agrees with the previous values given in Table IX.

TABLE X. COMPARISON OF THE OBSERVED AND CALCULATED MEAN AMPLITUDES (FOR PAIRS INCLUDING HYDROGEN) (in Å unit)

Pairs	Observed	Calculated
(C-C)	$0.052_6\pm0.003$	0.050_3
C-H	$0.083_1\pm0.004$	0.078_3
C-H (nonbonded)	$0.097_3\pm0.005$	0.109_7
H-H (nonbonded)	—	0.126_8
H-H (*trans*)	—	0.128_2
H-H (*gauche*)	—	0.156_8

The comparison of the calculated amplitudes with the observed values is given in Table IX and X. The agreement is satisfactory, taking account of the experimental error, and of the uncertainty in the theoretical values (possibly a small

58) J. C. Decius, *J. Chem. Phys.*, **16**, 1025 (1948).
59) S. Mizushima, T. Shimanouchi, I. Nakagawa and A. Miyake, ibid., **21**, 215 (1953).
60) T. Shimanouchi, *Sci. Papers Inst. Phys. Chem. Research (Tokyo)*, **40**, 467 (1943); *Bull. Inst. Phys. Chem. Research (Tokyo)*, **23**, 371 (1944).
61) M. Hayashi, *J. Chem. Soc. Japan, Pure Chem. Sec. (Nippon Kagaku Zasshi)*, **78**, 222 (1957).
62) Y. Morino, K. Kuchitsu and T. Shimanouchi, *J. Chem. Phys.*, **20**, 726 (1952).
63) Y. Morino, K. Kuchitsu, A. Takahashi and K. Maeda, ibid., **21**, 1927 (1953).
64) R. S. Rasmussen, ibid., **16**, 712 (1948).
* Although Gates (Ref. 15) assigned the Raman line 319 cm^{-1} to the lowest A_g mode, this line should be assigned to the same mode of the *gauche* form (Ref. 16). The valence force constants determined by Gates are therefore not very reliable.
65) I. Nakagawa, *J. Chem. Soc. Japan., Pure Chem. Sec. (Nippon Kagaku Zasshi)*, **74**, 848 (1953); **75**, 60 (1954).

percentage), caused by the approximate nature of the calculation, the uncertainty in the force constants, and the neglect of anharmonicity in the vibration.

Analysis of the Intensity in the Small-angle Region

The intensity curve in a small-q region was analyzed for the purpose of obtaining further information on the rotational isomerism. The detail of the method was described in a previous paper[19,66].

Diffraction photographs were taken at the longer camera length through an r^2-sector with a multiple-layer stopper of the same type as that used by Bastiansen[23]. The density measured was converted into the intensity by Karles' procedure[26]. Independent observations gave good agreement with one another.

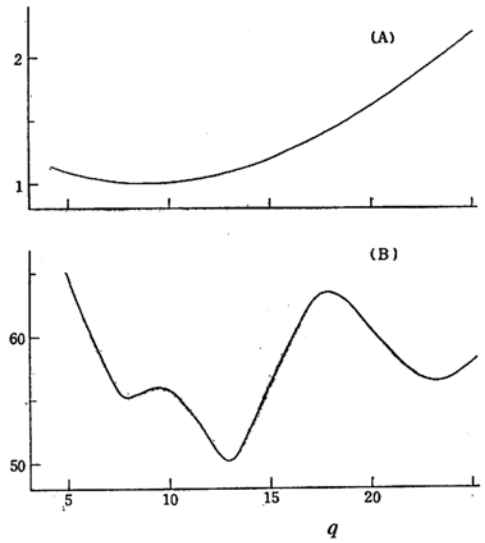

Fig. 12. Small-angle intensity curve of *n*-butane. (A) $f(q)$ curve; and (B) $f(q)I(q)$ curve.

The intensity $I(q)$ was multiplied by a smooth function $f(q)$ (Fig. 12) to make the background line nearly flat, where

$$f(q)=1+0.0054(q-9)^2+3\times10^{-6}(q-9)^4 \quad (62)$$

A background function $I_b(q)$ was calculated by the following equation,

$$I_b(q)=f(q)I(q)/(1+cM(q)_{\text{calc}}) \quad (63)$$

where $M(q)_{\text{calc}}$ is the theoretical molecular intensity divided by q, and c is the index of resolution[34,44]. A criterion that I_b should be a smooth function of q can be used to select a reasonable model[19].

The frame structure and the mean amplitudes determined by the analysis described on pages 750~757 was used to compute the theoretical molecular intensity, together with the same assumption discussed in *procedure* of that section. Two parameters of the rotational isomerism, the *gauche* azimuthal angle ϕ and the fraction of the *trans* form n_t, were varied systematically. The index of resolution was estimated to be 0.90±0.10.

It was found that when n_t was assumed to be less than 30% or more than 70%, the I_b functions (Fig. 13) showed such large fluctuations irrespective of the choice of angle ϕ, that the existence of both rotational isomers was definitely confirmed. It gives an independent support to the conclusion of the RD analysis.

For the estimation of the parameters and their limits, the maximum possible ripples caused by experimental errors or by theoretical uncertainties were regarded as about 1% of the I_b function*. The result of the analysis is

$$\phi=65°\pm10°, \text{ and } n_t=65\sim35\%$$

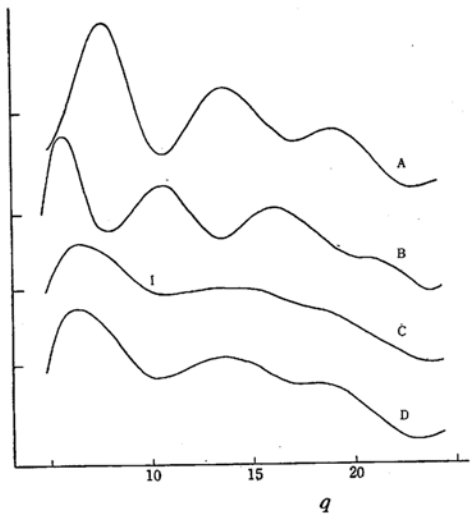

Fig. 13. I_b functions of *n*-butane for models (A) *trans* 100%; (B) *gauche* ($\phi=65°$) 100%; (C) a mixture of *trans* and *gauche* ($\phi=65°$) in 1:1; and (D) a mixture of *trans* and *gauche* ($\phi=50°$) in 1:1. The index of resolution is 0.90. The curve C is in the acceptable region. The vertical line denotes the amplitude of a one per cent fluctuation of the I_b curve.

66) K. Kuchitsu, This Bulletin, **30** 391, 399 (1957).

* This estimation was based on a similar argument given in the previous paper on *n*-propyl chloride (Ref. 19), but a larger value should be taken for the uncertainty in this case, since the contribution of the internal rotation is less (being about 20% of the total intensity), and the uncertainty of the assumptions is more serious (particularly for the position of the hydrogen atoms).

TABLE XI. COMPARISON OF THE STRUCTURES OF RELATED MOLECULES

Molecule	Ethane			Propane	Butane	
Method	Infrared	E.D.	E.D.	E.D.	E.D.	E.D.
C-H(A)	1.102	1.114±0.027	1.107	(1.09)	1.100±0.003	1.107_5±0.005
C-C(A)	1.543	1.536±0.016	1.536	1.54±0.02	1.53_9±0.003	1.533 ±0.003
∠C-C-H	109°37′	110.5°±3.5°	109°32′	—	110°22′±15′	110.5°±0.7°
∠C-C-C	—	—	—	111.5°±3°	112°9′±9′	112.4°±0.4°
Reference	3	4	5	7	Present work	72

E.D.: electron diffraction investigation.

which is consistent with the result on pages 750~757 within the limit of uncertainty.

Discussion

The C–H and C–C distances were obtained with accuracies of better than 0.01Å (Table VI). These distances are the average values of two non-equivalent distances, but they may not differ more than 0.01Å. It is seen that the values are close to the "normal" bond lengths[67] accepted generally: C–H=1.09Å, and C–C=1.54Å. This result therefore gives some support for these standard values.

The average C–C–H angle was found to be slightly larger than the tetrahedral angle. The structures of methyl groups have been obtained by means of microwave spectroscopy for a number of simple molecules[68]; the angles C–C–H differ slightly from one molecule to another around the tetrahedral angle.

The structural data for normal paraffins comparable with the present result are those for ethane and propane (Table XI). The spectroscopic value r_0 is slightly different from $r_g(0)$ (probably about 0.01Å or less), and the values given by electron diffration may be $r_g(1)$, although not stated explicitly. The general agreement shows that there may be no conspicuous difference between the structures of these hydrocarbons.

It was confirmed that the angle C–C–C is definitely larger than tetrahedral (112°9′). A similar but not so accurate result was obtained in propane (111.5°±3.5°)[7]. It is interesting to note that a similar fact was known for higher normal paraffin crystals studied by the X-ray diffraction; it was first noticed by Bunn[69], and confirmed in a recent study of Shearer and Vand[70], who found that ∠C–C–C=112°1′± 21′ for $C_{36}H_{74}$. This fact is consistent with the earlier theoretical prediction of Ingold[71] based on organic reactions.

As for the rotational isomerism, it was definitely confirmed that there are two isomers, the *trans* and the *gauche* forms, in the gaseous phase. The fractions of these forms were found to be about 60% for the *trans* form and about 40% for the *gauche* form. Since the complete assignment of the vibrational frequencies is not available at present, the partition functions can not be calculated. If the ratio of the functions is assumed to be unity, (the statistical weight for the *gauche* form being 2), then the energy difference between the two forms is about 650 cal./mol., the *trans* form being the more stable. This value is close to that of liquid *n*-butane[11,12], as expected. The azimuthal angle of the *gauche* form was found to be slightly larger than 60°. The effect of hindered internal rotation around the *trans* position was observed in the shift of the *trans* C–C distance. An evaluation of the barrier height gave a rough but reasonable order of magnitude for this value.

A precise measurement of the structure of *n*-butane has been made by Bartell[72]. His result is in satisfactory agreement with the present result, except slight discrepancies in atomic distances (less than 0.7%) which may be partly due to uncertainties in the scale factor.

Summary

The molecular structure of *n*-butane has been investigated by means of the sector-microphotometer method of electron diffraction. The least-square analysis of the radial distribution curve has been carried out both for modified and unmodified curves giving the internuclear

67) L. Pauling, "The Nature of the Chemical Bond", Cornell University Press, Ithaca, N. Y. (1940), p. 160.
68) W. Gordy, W. V. Smith and R. F. Trambarulo, "Microwave Spectroscopy", John Wiley and Sons, Inc., New York (1953). C. H. Townes and A. L. Shawlow, "Microwave Spectroscopy" McGraw-Hill, New York (1955).
69) C. W. Bann, *Trans. Faraday Soc.*, **35**, 482 (1939).
70) H. M. M. Shearer and V. Vand, *Acta Cryst.*, **9**, 379 (1956).
71) C. K. Ingold, *J. Chem. Soc.*, **1921**, 305.
72) L. S. Bartell, private communication (1958).

distances as well as their mean amplitudes and the bond angles. The estimation of experimental standard errors has been made by examining various sources of errors. Important results are the following:

a) The average distance of the C–C bonds is 1.539±0.003Å.

b) The angle C–C–C is 112°9′±9′, is considerably greater than the tetrahedral angle.

c) The position of hydrogen atoms is located with considerable accuracy; C–H =1.100±0.003Å and ∠C–C–H=110°22′±15′.

d) The mean amplitudes measured are in agreement with the calculated values within the limit of error.

e) The existence of rotational isomers, the *trans* and the *gauche* forms, are confirmed. The structure and the fraction of the isomers are determined. The result is consistent with the spectroscopic results.

The author wishes to express his sincere gratitude to Professor Yonezo Morino for his kind guidance and encouragement throughout this work. He is also indebted to Mr. H. Morimoto of Nagoya Univesity and to Dr. M. Iwasaki of the Government Industrial Research Institute of Nagoya for their help in the microphotometry, to Mr. R. Tsunoda in the Division of Health and Welfare Statistics, Welfare Ministries Secretariat for the use of the punched cards machines, and to Mr. T. Takatani of Hitachi Central Research Laboratory for his kind supply of the *n*-butane sample. This research was financially supported by the Scientific Grant from the Ministry of Education.

Department of Chemistry
Faculty of Science
The University of Tokyo
Hongo, Tokyo